Light Bullet Creation, Routing, and Control with Planar Waveguide Arrays

Matthew O. Williams*, Colin W. McGrath†, and J. Nathan Kutz ‡

Abstract— **A theoretical model of the mode-locking of light bullets in a planar slab waveguide array is presented. The model yields three dimensional localized solutions that act as global attractors for particular parameter values. The these solutions can be controlled via non-uniformities in the gain applied to the array. This manipulation is robust and allows for bullet routing as well as the production of the NAND and NOR logic gates.**

Keywords: mode-locking, waveguide arrays, light-bullets

1 Introduction

The technological feasibility and nonlinear properties of semiconductor waveguide arrays (WGAs) make them an ideal technology for all-optical signal processing applications. The property of WGAs that make them so attractive from a technological standpoint is that nonlinear self-focusing is capable of overcoming discrete spatial diffraction for a sufficiently intense electrical field. This was predicted theoretically by Christodoulides and Joseph [1] and later shown experimentally by Eisenberg et al. [2]. Based on this work, the WGA was proposed as an ideal component for both optical routing and switching purposes [2–5], temporal mode-locking of lasers [6–9], and the generation of spatial optical solitons [1–5].

In this manuscript, the generation of three-dimensional spatial confinement is based on the generation of temporal solitons in the WGA structure. Due to the planar structure of the waveguides in this slab waveguide array mode-locking model (SWGAML), the nonlinear mode coupling that creates temporal solitons in the WGA will generate the spatial confinement needed for light-bullet formation [10–12]. In addition to the generation of bullets, we propose further enhancements to the SWGAML that allow the control and routing of bullets produced in the slab waveguide structure [14, 15].

*University of Washington, Department of Applied Mathematics, Seattle WA USA 98195-2420 Tel/Fax: 206-685-3029/1440 Email: mowill@amath.washington.edu

†University of Washington, Department of Applied Mathematics, Seattle WA USA 98195-2420 Tel/Fax: 206-685-3029/1440 Email: waffle20@u.washington.edu.

‡University of Washington, Department of Applied Mathematics, Seattle WA USA 98195-2420 Tel/Fax: 206-685-3029/1440 Email: kutz@amath.washington.edu

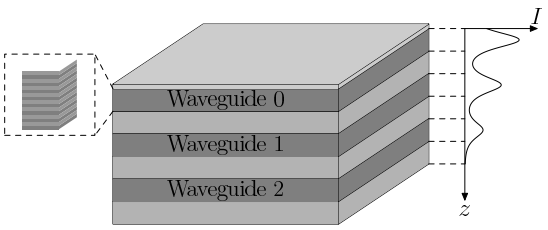

Figure 1: Schematic of a slab waveguide array theoretically capable of producing light-bullets. Slab waveguides (gray) are separated by light-gray non-guiding regions to produce a weak coupling between adjacent arrays. Gain is applied to the topmost waveguide via current injection.

The outline of the paper is as follows: In Sec. 2, a description of the physical system is given. In Sec. 3, the governing equations and the parameters in the model are given. In Sec. 4, the creation and stability of light bullets are discussed for uniform gain profiles. In Sec. 5, bullet routing and control using non-uniform gain profiles are demonstrated. In Sec. 6, the interactions of multiple bullets are used to produce the NAND and NOR gate. Lastly, Sec. 7 contains some concluding remarks and technological outlook for the WGA device and its applications.

2 System Description

The proposed device is a slab waveguide array consisting of three waveguides, as shown in Fig. 1. The three planar slab waveguides are labeled zero through two from the top of the device to the bottom respectively. Non-guiding regions are placed between the individual waveguides to weaken the coupling between adjacent waveguides. Gain could be provided to the system through a monolithic gold layer attached to the zeroth waveguide [13]. This layer allows for the injection of current into the zeroth waveguide but does not inject current into any of the other two. One modification useful for applications is to partition the gold layer as in [15]. By injecting different amounts of current into individual partitions, a non-uniform gain profile is generated in the system. The uses of these extra degrees of freedom will be explored later in this manuscript.

This device is envisioned to operate like a VCSEL, so the

phase velocity of light is in the vertical direction as shown in Fig. 1. The light bullets themselves are stationary in space and confined in each of the waveguides. This geometrical structure extends the idea of the nonlinear mode coupling (NLMC) [9, 16] so critical in temporal mode-locking from a single dimension to the pair of dimensions in the plane of the waveguide. This extension confines the bullet in the plane. In order to have a stationary bullet, a third dimension of confinement is required. The third dimension of confinement is assumed to be created by the structure of the array in the remaining spatial dimension.

There are a number of current technologies capable of generating the additional dimension of confinement. One particular example is the zero group velocity soliton, which has been obtained theoretically and is the target of ongoing experimental work [17, 18]. Another option, particularly suited to the WGA, is the use of defects in Bragg gratings to trap Bragg solitons [19]. By replacing the guiding regions with Bragg gratings and using the insulating regions as defects the geometrical structure of the WGA itself should be sufficient to generate a trapped Bragg soliton.

Either of the previous two mechanisms would be sufficient to create effectively zero-group velocity bullets. Since the interaction of solitons in the adjacent waveguides is modeled via coupled mode theory [20], the exact mechanism is not important to the overal structure of the governing equations. The slab waveguide mode-locking model (SWGAML) discussed in the next section is robust enough to capture both situations. The combination of these two effects, NLMC in the plane of the waveguide and the Bragg or gap-soliton in the normal direction, is sufficient to produce confinement in all three spatial dimension resulting in what we are calling a light-bullet. As will be shown, these light bullets act as global attractors to the system and will therefore form naturally from a cold cavity.

3 Governing Equations

Mode-locking in waveguide arrays is created by a competition between the saturable absorption generated by NLMC [9] of the waveguides and the bandwidth limited gain. The waveguide array mode-locking model (WGAML) [8] describes the temporal mode-locking in traditional ridge waveguide arrays. To model this slab waveguide system, the WGAML was heuristically extended from one to two spatial dimensions:

$$i\frac{\partial A_0}{\partial t} + \frac{D}{2}\nabla^2 A_0 + \beta|A_0|^2 A_0 + CA_1 + i\gamma_0 A_0 - ig(x,y,t)(1+\tau\nabla^2)A_0 + i\rho|A_0|^4 A_0 = 0 \quad (1a)$$

$$i\frac{\partial A_1}{\partial t} + C(A_0 + A_2) + i\gamma_1 A_1 = 0 \quad (1b)$$

$$i\frac{\partial A_2}{\partial t} + CA_1 + i\gamma_2 A_2 = 0 \quad (1c)$$

where $\nabla^2 = \partial_x^2 + \partial_y^2$. The impact of current injection is modeled as a saturating gain:

$$g(x,t,y) = \frac{2g_0 f(x,y)}{1 + ||A_0||^2/e_0}. \quad (2)$$

In (1), A_0, A_1, and A_2 are the envelopes of the electric fields in the 0th, 1st, and 2nd waveguides respectively. Unlike the WGAML [8], the SWGAML is in a stationary frame and so D is the diffraction coefficient where the sign of D is the sign of the index of refraction. β determines the strength of the Kerr nonlinearity, ρ is proportional to the probably of three photon absorption occurring, the γ_j are the aggregation of linear losses for each waveguide, and C is the strength of evanescent coupling between adjacent waveguides. The saturable gain $g(x,y,t)$ accounts for the depletion of minority charge carriers at high optical intensities, resulting in a saturating gain. The filtering term, $g\tau\nabla^2$ results in higher frequency spatial modes receiving lower amounts of gain than lower frequency modes. This term can be though to arise from diffusion which results in more explicit models of the gain medium [21].

The function $f(x,y,t)$ in (2) accounts for the possibility of non-uniform gain profiles. In order to uniquely specify the gain, it is imposed that the mean of $f(x,y,t)$ is one at all times and $f(x,y,t) \geq 0$. Therefore, larger values of g_0 always correspond to larger total injection currents regardless of the exact form of $f(x,y,t)$. The addition of non-uniform gain allows for a variety of additional dynamics not found in the uniform gain case. In particular, a non-uniform gain breaks translational invariance in the system and creates solutions where the bullets translate in space.

4 Uniform Gain Dynamics

The study of the uniform gain dynamics in an important first step in describing the SWGAML. With uniform gain, $f(x,y,t) = 1$ and there are two distinct asymptotically stable types of mode-locked solutions – stationary solutions and breather solutions. For both types of solutions, the system can have an arbitrary number of bullets, e.g., a double bullet stationary solution. In this section, we explore these types of solutions and their dependence on the total gain, g_0, applied to the system.

4.1 Stationary Light-Bullets

The first type of mode-locked solution is the stationary bullet solutions which have constant amplitudes in time. With uniform gain,the SWGAML is a radially symmetric system of equations. Although non-radially symmetric solutions could exist, the radially symmetric solutions are of lower energy and are therefore the favored solutions when starting from a cold cavity. The radial symmetry can be exploited to remove a spatial dimension from the

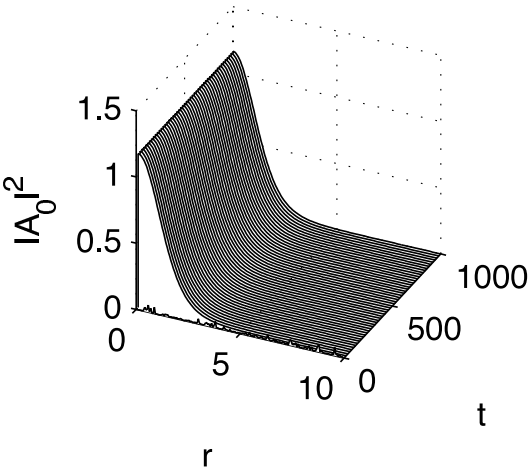

Figure 2: Example of a radially symmetric stationary solution with the parameters from (3). The initial condition is noise in the zeroth waveguide and zero in the other two waveguides. The radially symmetric bullet solution forms from noise and appears to be a global attractor of the system.

problem allowing for faster and more accurate simulations. Figure 2 shows an example of a radially symmetric solution obtained with

$$(D, C, \gamma_0, \gamma_1, \gamma_2, e_0, \tau, \rho, g_0) = (-1, 10, 0, 0, 10, 1, 0.1, 1, 35) \tag{3}$$

The system quickly settles into a steady state starting from noisy initial conditions. To obtain this result, a finite difference scheme was used with Neumann boundary conditions at the origin. The computational domain uses is larger than that shown in Fig. 2 so the Dirichlet boundary condition used at the far end is unlikely have caused a major impact on the resulting dynamics.

For the particular parameters chosen, this solution appears to be the only stable attractor in the system. In previous works [8, 22] on the one dimensional WGAML, it has been shown that another branch of low amplitude solutions exist. The software package AUTO [23] was used to track the branch of stationary solutions using a finite difference approximation to compute the derivatives. This coarse approximation to the function was used as a starting point for a more accurate calculation using a Chebyshev collocation method [24]. This collocation method approach allows for the eigenvalues of the linearized operator to be computed with spectral accuracy. Errors in the eigenvalue are estimated to be on the order of 10^{-8}. This combined approach was used to generate the bifurcation diagram and example spectra in Fig. 3 for the stationary solutions. In Fig. 3, black regions are linearly stable and gray regions are linearly unstable. It is clear that a saddle-node bifurcation is responsible for the creation of the single-pulse solution. The maximum amplitude of the pulse is directly related to the gain pro-

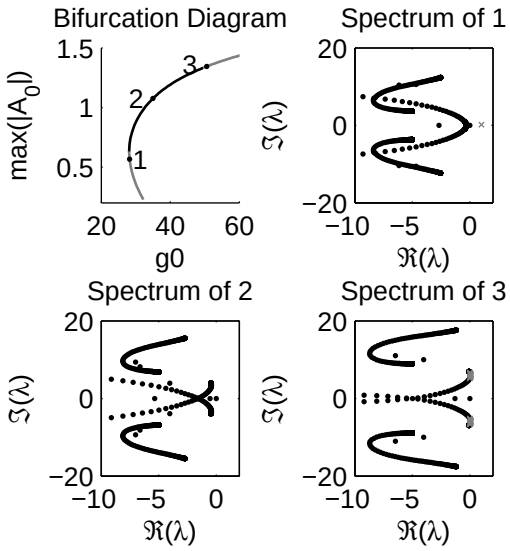

Figure 3: The bifurcation diagram and spectrum of selected radially symmetric bullet solutions. In the bifurcation diagram, the black curve is where the bullet is linearly stable while the gray regions are where it is not. In the spectra, gray xs represent eigenvalues with positive real parts. Light bullet solutions are born out of a saddle node bifurcation near point 1 and go unstable near point 3 due to a Hopf bifurcation.

vided to the system, but around $g_0 = 50$ a Hopf bifurcation occurs and the periodic breather solutions become the stable solutions.

4.2 Time-Periodic Breather Solutions

Due to the Hopf bifurcation, it is known that time-periodic breather solutions occur for some range of the bifurcation parameter g_0. While more complicated than the stationary solutions, breather solutions contain both a larger peak intensity and a larger total energy and may be useful in applications where these traits are desired and a stationary bullet profile not required.

Figure 4 shows an example of a time-periodic breather solution using the parameters:

$$(D, C, \gamma_0, \gamma_1, \gamma_2, e_0, \tau, \rho, g_0) = (-1, 10, 0, 0, 10, 1, 0.1, 1, 50). \tag{4}$$

All the parameters except for g_0 are the same as the single bullet case. In Fig. 4, it was assumed that the periodic solutions were also radially symmetric. However, in full two-dimensional simulations it was found that a low amplitude non-radial background occurs in addition to the central radial bullet [25]. This non-radial component is never captured by the radial solution approximation. It is unclear whether or not this non-radial background is inherent in the PDE or is a result of the periodic boundary conditions and square domain imposed in the two-dimensional problem. However, in both the radially sym-

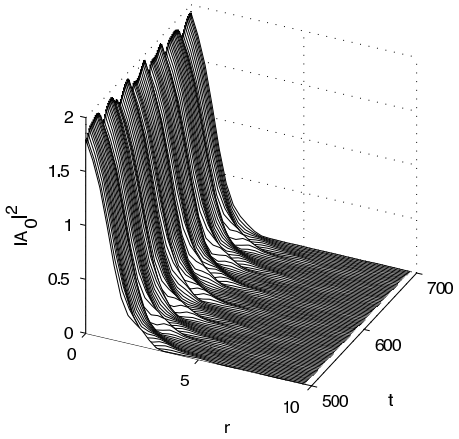

Figure 4: The amplitude in the zeroth waveguide as a function of time for a time-periodic breather solutions using the parameters in (4). At higher gains, the stationary solution is unstable and the breather solution the dominant solution time.

metric case and the full PDE the results are qualitatively similar. If quantitative predictions of bullet dynamics are required, the radially symmetric approximation is no longer valid for the parameters used in simulation.

4.3 Multiple-Pulse Solutions

At larger gains, the breather solution loses stability and a stationary solution with a larger number of bullets dominates. These stationary solutions are essentially equivalent to the single-bullet solutions in Sec. 4.1. In all of the simulations run, final solution has been two non-interacting stationary bullets. This is similar to what has been seen in the one-dimensional WGAML [8].

While the final state of the solution is quite simple, the route taken from a single to a double bullet is complicated and the transition may persist for long periods of time. Figure 5 shows the time evolution of a solution that splits. The initial condition is a single stationary solution bullet, but gain is too large for the stationary or even breather solutions to be stable. The bullet then radiates energy and eventually a second bullet forms from the energy travelling around the periodic domain. If the second bullet forms in close proximity to the existing bullet, the bullets will recombine into a single unstable bullet which starts the splitting process over again. Ultimately, this process results in two bullets sufficiently separated that they will not recombine. For this reason, the multiple bullet solution may be treated as a number of single non-interacting bullets.

The splitting process in Fig. 5 appears to be chaotic in nature and the SWAGML may remain in this chaotic state for protracted periods of time. Note that the 160 time units in Fig. 5 is shorter than the typical amount of

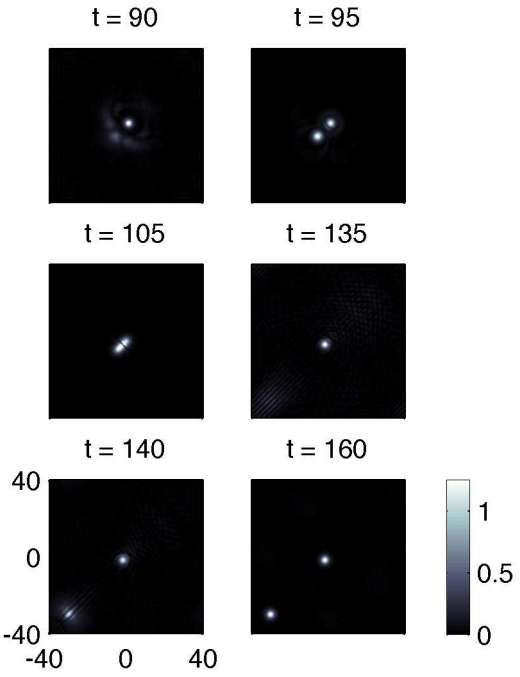

Figure 5: Time evolution of the splitting of a single light bullet into a pair of light bullets. Due to the larger gain, the single pulse sheds energy which eventually results in the formation of a second pulse. Note that the resulting bullets are far separated in space. If the second bullet forms in close proximity, it will interact with the original bullet and be absorbed which repeats the splitting process.

time requires for bullets to split. For many parameters, this transition process may exist for over a thousand time units and is heavily dependent on the initial condition. In many ways, despite the presence of structures in the plane of the waveguides the splitting process is chaotic in nature.

It should be noted that it is possible to form stationary solutions where the bullets do interact. For identical bullets, separations have been found where the relative phase difference between the bullets determines whether or not the pair persists or recombines. However, this situation has only occurred when very specific initial conditions are employed and never when a single bullet was used as the initial conditions. Therefore, the multiple bullet solutions can be treated as a pair of non-interacting single bullets as those are the only types of solutions that have been observed in numerical experiments studying the splitting process. While solutions with interacting bullets do exist, in this work as well as in previous works [15,25] these solutions have never appeared except from very specific initial conditions.

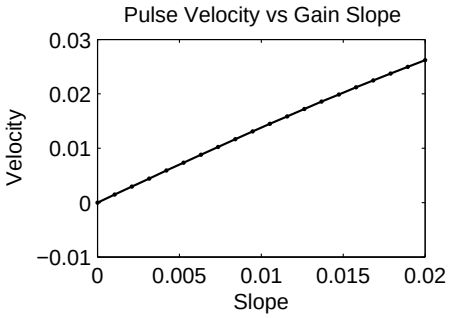

Figure 6: Plot of the velocity of the bullet as a function of the slope of the gain profile. The velocity of the bullet is directly related to the slope of the gain. Furthermore, for sufficiently small gain ramp the velocity is linearly related to gain.

5 Non-Uniform Gain Dynamics

Using $f(x, y, t) = 1$, the governing equations (1) contain a number of symmetries, including translational invariance. The translational invariance eliminates the possibility of creating a single spatial location that attracts bullets in the array. In experimental works on similar systems [12], external lasers were used to pump the system and manipulate the location where bullets formed. A similar effect can be obtained in this system using variations in the current injected to the system.

5.1 Constant Gain Slope

The simplest non-uniform gain profile is a linearly sloped gain profile. In this work, the slopes of the gain profile were kept small. This restriction serves two purposes. First, the use of small slopes allows the non-uniformity to be considered a perturbation of the uniform case. In this regime, the branches of solutions obtained in Fig. 3 will remain valid to leading order. Therefore, the solutions from the uniform case can be use as initial conditions without a large amount of transient behavior resulting. Second, the inclusion of large gain slopes often creates regions with large enough gain that a second bullet simply forms in that region, annihilating the first bullet. Although there is no inherent technological limitation to small gain slopes and this type of motion may be physically realistic, this type of motion is more difficult to control and will not be considered in this manuscript.

Figure 6 shows that the velocity of the light bullet is directly related to slope of the gain. For the small slopes used, the bullet is not noticeably deformed from the stationary bullet case. Additionally, the bullet trajectory is the same as the gradient of the gain function, and there is no spurious motion in any other direction. The ramped gain case can serve the conceptual starting point for more complex gain profiles, and it provides a simple mechanism for imparting velocity onto the light-bullets. For more complex behaviors, one approach is to use piecewise linear functions to trace out paths in the plane.

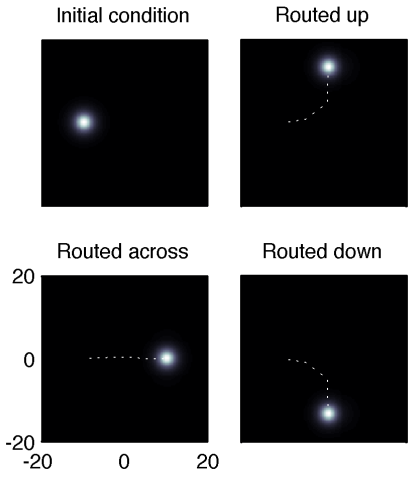

Figure 7: Bullet routing using the gain equation in (5). The dotted lines show the location of the bullet center as time progresses. The piecewise linear gain routes the bullet through the junction.

5.2 Bullet Routing with Sloped Gain

The use of sloped gain generates a simple method of bullet routing. As shown in Sec. 5, bullets gain velocity in the direction of the gradient of the gain. The simplest types of functions would be comprised of piecewise linear functions. These functions are capable of a robustly routing bullets even through large angles.

As an example, a junction can be created generating a single gain ramp but superimpose it with forbidden regions that contain no gain. Mathematically, gain was modelled as

$$f(x, y, t) = \begin{cases} (1 + mx + ny) & |x| < 8 \text{ or } |y| < 8 \\ 0 & \text{otherwise} \end{cases} \quad (5)$$

where m and n control the direction in which the bullet moves. The result is a plus-shaped junction where one arm is the input and the other three outputs. Directing the light bullets is done simply by changing the value of m or n which control the direction of the slope of the gain. Figure 7 shows the three possible routings with $m = 0.01$. The final bullet location is chosen by the value of n. When $n = 0.01$ the bullet is routed up, when $n = 0$ the bullet is routed across, an when $n = -0.01$ the bullet is routed downward.

In the application of a piecewise linear gain, the regions of zero gain in Fig. 7 prevent the bullet from entering the region and do not destroy or trap the incoming bullet. The result is the bullet being routed through the junction rather than taking the most direct path between the

outputs. The inclusion of these regions creates great flexibility in the generation and construction of devices used for bullet routing.

5.3 Time Dependent Gains

Stationary gain profiles are the simplest to construct but have inherent limitations due to their stationary nature. As an example, stationary gain profiles are unable to manipulate light-bullets into a time-periodic orbit. For small enough gain slopes, light-bullets follow the gradient of the gain function. However, no continuous function can have a closed orbit with an always increasing gradient. Additionally as shown in Sec. 5.2, the solutions to the SWGAML have effectively no momentum so the discontinuity cannot be overcome.

However, time-periodic orbits can be obtained by using a time-periodic gain function. The simplest case is a gain profile that translates in time but is otherwise stationary in time such as the following Gaussian profile:

$$f(x,y,t)=\exp\left(-\alpha\Big([x-10\cos\omega t]^2+[y-10\sin\omega t]^2\Big)\right) \quad (6)$$

where numerically $\alpha = 0.001$ and $\omega = 2\pi/5000$. The angular frequency of movement, ω, is small relative to the timescale that dynamics typically occur on in the SWGAML. This is consistent with most physical systems where gain manipulations occur on much slower timescales than the evolution of the bullets.

Due to the slow translation of the gain the movement of the bullet can be thought of as an adiabatic process. For any position of the gain, the bullet has sufficient time to follow the gain gradient to the maximum of the gain profile. As the gain translates, this process repeats. The effect is a light bullet that is bound to the top of the translating gain profile and follows a path nearly identical to the moving gain. This process is shown for the Gaussian profile in Eq. 6 in Fig. 8.

In Fig. 8, the x and y position of both the bullet and the gain are shown for a variety of times. In order to determine the bullet center, the following formulas were used for both the bullet and the gain:

$$\text{bullet center}=\frac{\iint x|A_0|^2dxdy}{||A_0||^2}\hat{x}+\frac{\iint y|A_0|^2dxdy}{||A_0||^2}\hat{y}. \quad (7)$$

As the gain is a radially symmetric solution and bullet is to leading order a radially symmetric solution, this formula accurately describes the centers of both functions. The bullet and gain overlap to a significant degree. There is a slight lag between the centers of the gain and the bullet since this process is not completely adiabatic. Nonetheless, it is clear these translating gains can manipulate light bullets in time-periodic orbits and indeed any arbitrary continuous path. Since the current injected into the system is controlled by external electronics, these same external electronics indirectly provide a mechanism for bullet routing and control.

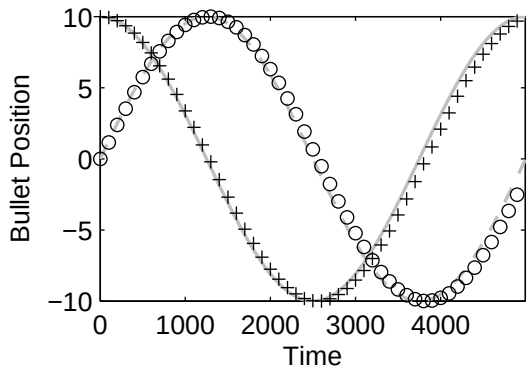

Figure 8: Bullet control using time dependent gain. The + and ∘ show the x and y coordinates of the bullet center as a function of time. The gray lines show the x and y coordinates of the gain function in (6) as a function of time.

6 Gain Mediated Interactions

In Sec. 4.3, it shown that the SWGAML is capable of supporting multiple-bullet solutions. By employing non-uniform gain profiles as in Sec. 5, it is possible to route both of the bullets simultaneously. Therefore, it is possible to make use of multiple bullets and their interactions. The interaction of multiple bullets occurs through two distinct processes. The first is a direct interaction when two bullets are physically close enough to interact, similar to the interactions seen in the nonlinear Schrödinger equation [26]. Similar to NLS, the resulting dynamics of the interaction depends heavily on the separation of the two bullets as well as the relative phase difference between them. The resulting dynamics is therefore heavily influenced by the initial condition of the SWGAML.

In the applications envisioned for this device, it is unlikely one would be able to guarantee a particular phase-difference. The simpler and more robust of the interactions are gain-mediated interactions. These types of interactions occur only through the gain term in (2). In the gain term, the level of saturation is determined by the L^2 norm. This non-local term allows bullets that are physically separated to influence one-another by increasing or reducing the gain of the system. While less powerful than direct interactions, this mechanism is still capable of producing both the NOR and NAND logic gates and would therefore be useful in applications.

6.1 NOR Gate

The first of the two master-gates implemented in the SWGAML is the NOR gate. The NOR gate has up to three inputs. The clock bullet must always exist in the

system, but the input bullets will only exist if that particular input is a logical high input. The NOR gate is produced using three stationary gain ramps which route both input bullets and well as a clock bullet from the input of the NOR gate to the output. If the clock bullet reaches the output of the gate, then the result is logical high. Otherwise, the output is logical low.

What differentiates this from the bullet routing shown in previous sections is that, while there are three bullets, the system is given sufficient gain to support only a single bullet. Therefore, all three of the bullets will decay. To select which of the three bullets survives, each of the gain ramps is given different amounts of gain. Specifically, the clock bullet ramp receives less gain than either of the two input bullets. From the stability results of Fig. 3, a slightly reduced gain is not of consequence in the long run because single bullets are stable for a range of gains.

If the clock bullet is the only bullet in the system, it will have enough gain to persist and translate to the output. If any of the two input bullets are introduced to the system, then all of the bullets will decay. Due to the lower gain given to the clock bullet, it will decay faster than either of the input bullets. Therefore, it will always be destroyed if any of the inputs exist. This is consistent with a NOR gate.

Figure 9 shows each of the four possible scenarios for the NOR gate. Because these interactions are completely gain mediated, this process does not require any partic-

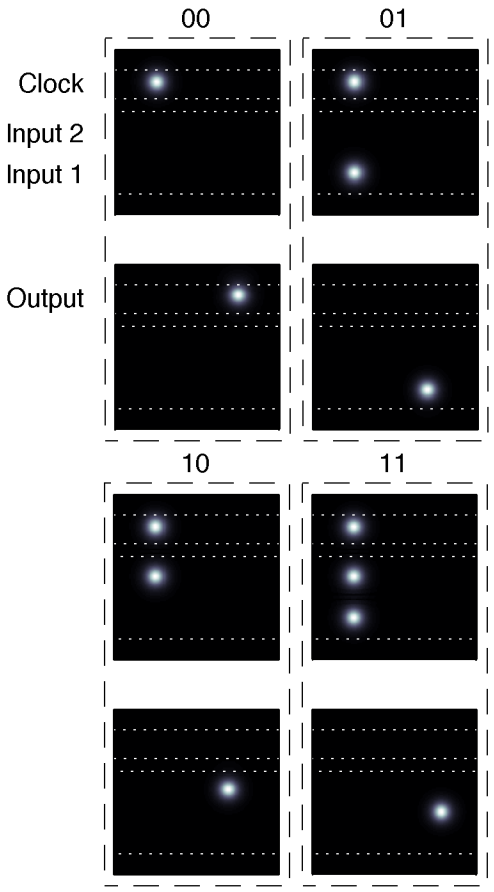

Figure 9: A plot of all possible cases for the NOR gate. Both the clock and input bullets experience a sloped gain which routes all bullets from left to right. Gain is biased so the clock receives less gain than either of the input bullets. The system possesses enough gain to support a single bullet so the clock bullet will be destroyed if either input bullet exists. If neither exist, the clock bullet translates right giving a high output.

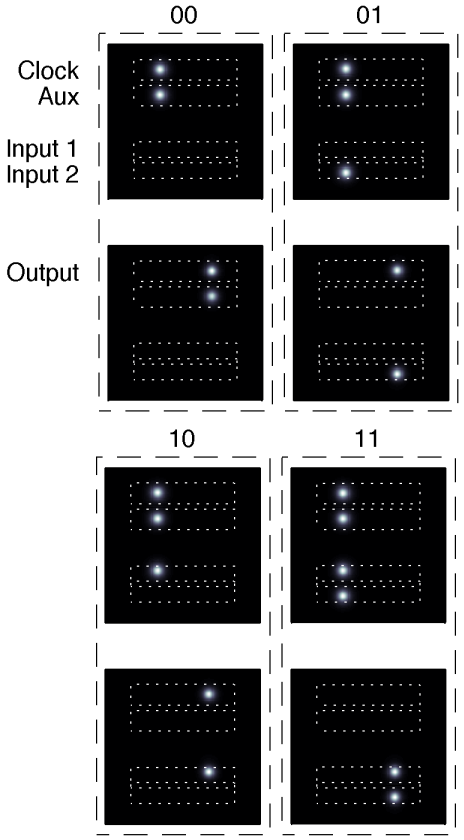

Figure 10: Four possible cases for the NAND gate. Note that each of the four possible bullets experiences a time periodic gain similar to (6) that translates the bullet from left to right. However, the overall gain given to each bullet, from lowest to highest, is: the auxiliary bullet, the clock bullet, the input one bullet, and the input two bullet. The NAND gate has enough gain to support a pair of bullets so if at most one of the inputs bullets exist the output is high. Otherwise, the output is low.

ular phase difference between the input bullets to exist. Furthermore, while both of the input bullets in Fig. 9 received the same gain, that need not be the case. As long as the clock bullet receives less gain than either of the two input bullets, the result will be a NOR gate similar to what is shown in Fig. 9 although the results at the final time may be different.

6.2 NAND Gate

The SWGAML can also implement the NAND gate. In contrast to the NOR gate, this gate has been produced using time-dependent gains similar to Sec. 5.3. For the NAND gate, a Gaussian profiles is used to translate the clock bullet, the auxiliary bullet, and any of the input bullets. Figure 10 enumerates the four possible cases for the NAND gate. As shown, the NAND gate is comprised of up to four bullets. The clock bullet and auxiliary bullet must exist regardless of inputs. There are additionally up to two additional input bullets, depending on the inputs to the gate. The gain profiles exist whether or not either of the two inputs exists. Therefore, this NAND gate does not require any prior knowledge about the inputs.

Like the NOR gate, the key to constructing a NAND gate is to provide insufficient gain for all the bullets and to use differences in the gain to select in which order bullets are destroyed. For the NAND gate, enough gain for two bullets is provided and the level of gain provided to each of the bullets is, from highest to lowest, input two, input one, the clock bullet, and the auxiliary bullet. If neither of the inputs exist, there is enough gain to support both the clock and auxiliary bullets . Therefore, they will translate to the output. Since the clock bullet reaches the output, this is a logical high. If one input exists, all three bullets will decay. As the auxiliary bullet has the lowest gain, it will be destroyed before the clock or input bullet. At that point, the clock and input bullets translate to the output and again logical high is the output. The final case is if there are two input bullets. In this case, the ordering of gain causes both the clock and auxiliary bullets to be destroyed resulting in the output being logical low. These four cases are consistent with the four possible cases of the NAND gate.

In principal, the NAND gate could be constructed with the same static gain profiles the NOR gate was constructed with, and the NOR gate could be constructed using the same time-dependent gains the NAND gate was constructed with. Furthermore, an auxiliary bullet could be added to the NOR gate using the same gain ordering as the NAND gate but with only enough gain for a single bullet. Using a simple change in the overall level of gain it is possible to convert a NOR gate to a NAND gate and vice versa with no other external changes to the system.

Although the other gates will not be constructed in this manuscript, the generation of the two master gates shows that fully operational photonic logic devices can be constructed. Since the output of each device is a light-bullet capable of serving as an input to an additional gate and since the NAND and NOR gates are insensitive to small delays in the input bullets, generating larger photonic circuits from these building blocks is trivial, and the other gates can be easily realized through combinations NAND and NOR. Therefore, it is possible to do photonically in the SWGAML any computation that could be done digitally.

7 Conclusions and Future Work

Light bullets hold tremendous potential as a critically important technology in the field of photonics and a number of research groups are focusing on this technology [10–12,15,25,27–37]. There are numerous technological methods both proposed and realized for engineering and controlling light bullets, and our approach is certainly not the only viable option for producing light bullets. However, as with all technologies, the implementation of light bullet technology requires the system to be both robust and inexpensive. Using slab waveguides, we have theoretically shown the ability of the SWGAML to produce and stabilize light bullets starting from noise. Furthermore, with the introduction of non-uniform gains these light bullets can be routed. Light bullets that are routable may be brought in close enough proximity to interact via gain. Gain mediated interactions are capable of reproducing the master logic gates and therefore all logic gates. Furthermore, the SWGAML architecture relies on simple input and output coupling as well as easily addressable routing via modulations of the gain provided to the system. Therefore, the SWGAML is able to control all-optical data streams and is capable of doing so in a feasible and easy to implement manner.

Acknowledgements

J. N. Kutz acknowledges support from the National Science Foundation (DMS-0604700) and the Air Force Office of Scientific Research (FA9550-09-0174).

References

[1] Christodoulides, D. N., Joseph, R. I. "Discrete self-focusing in nonlinear arrays of coupled waveguides," *Opt. Lett.*, V13, pp. 794-796, 1988.

[2] Eisenberg, H. S., Silberberg, Y., Morandotti, R., Boyd, A. R., and Aitchison, J. S. "Discrete spatial optical solitons in waveguide arrays," *Phys. Rev. Lett.*, V81, pp. 3383-3386, 1998.

[3] Aceves, A. B., De Angelis, C., Peschel, T., Muschall, R., Lederer, F., Trillo, S., and Wabnitz, S. "Discrete self-trapping, soliton interactions, and beam steering

in nonlinear waveguide arrays," *Phys. Rev. E*, V53, pp. 1172-1189, 1996.

[4] Eisenberg, H. S., Morandotti, R., Silberberg, Y., Arnold, J. M., Pennelli, G., and Aitchison, J. S. "Optical discrete solitons in waveguide arrays. i. soliton formation," *J. Opt. Soc. Am. B*, V19, pp. 2938-2944, 2002.

[5] Peschel, U., Morandotti, R., Arnold, J. M., Aitchison, J. S., Eisenberg, H. S., Silberberg, Y., Pertsch, T., and Lederer, F. "Optical discrete solitons in waveguide arrays. 2. dynamic properties," *J. Opt. Soc. Am. B*, V19, pp. 2637-2644, 2002.

[6] Kutz, J. N. *Mode-Locking of Fiber Lasers via Nonlinear Mode-Coupling*, volume 661 of *Lecture Notes in Physics*. Springer Berlin / Heidelberg, 2005.

[7] Proctor, J. and Kutz, J. N. "Theory and simulation of passive mode-locking with waveguide arrays," *Optics Letters*, V13, pp. 2013-1015, 2005.

[8] Kutz, J. N. and Sandstede, B. "Theory of passive harmonicmode-locking using waveguide arrays," *Opt. Express*,V16, pp. 636-650, 2008.

[9] Bale, B. G., Kutz, J. N., and Sandstede, B. "Optimizing waveguide array mode-locking for high-power fiber lasers," *Photonics North 2009*, V7386, pp. 73862W, 2009.

[10] Silberberg, Y. "Collapse of optical pulses," *Opt. Lett.*, V15, pp. 1282-1284, 1990.

[11] Wise, F. and Trapani, P. D. "The hunt for light bullets – spatiotemporal solitons," *Optics and Photonics News*, V13, pp. 28-32, 2002.

[12] See the Fundamentals, Functionalities, and Applications of Cavity Solitons (FunFACS) webpage for a complete overview of current and potential methods and realizations of generating localized optical structures: www.funfacs.org.

[13] Williams, M. O., Feng, M., Kutz, J. N., Silverman, K., Mirin, R., and Cundiff, S. "Intensity dynamics in semiconductor laser arrays," *OSA Nonlinear Optics 2009 Technical Digest*, JTuB14, 2009.

[14] Williams, M. O., Kutz, J. N., "Light Bullet Mode-Locking In Waveguide Arrays," Lecture Notes in Engineering and Computer Science: Proceedings of The International MultiConference of Engineers and Computer Scientists 2010, IMECS 2010, 17-19 March, 2010, Hong Kong, pp. 1315-1320

[15] Williams, M. O., McGrath, C. W., and Kutz, J. N. "Light-bullet routing and control with planar waveguide arrays," *Opt. Express*, V18, pp. 11671-11682, 2010.

[16] Hudson, D., Shish, K., Schibli, T., Kutz, J. N., Christodoulides, D., Morandotti, R., and Cundiff, S. "Nonlinear femtosecond pulse reshaping in waveguide arrays," *Opt. Lett.*, V33, pp. 1440-1442, 2008.

[17] Marangos, J. "Slow light in cool atoms," *Nature*, V397, pp. 559-560, 1999.

[18] Mok, J. T., de Sterke, C. M., Liter, I. C. M., and Eggleton, B. J. "Dispersionless slow light using gap solitons," *Nature Physics*, V2, pp. 775-780, 2006.

[19] Chen, P. Y. P., Malomed, B. A., and Chu, P. L. "Trapping bragg solitons by a pair of defects," *Phys. Rev. E*, V71, pp. 066601, 2005.

[20] Yariv, A. *Quantum Electronics*, John Wiley and Sons, 1988.

[21] Rahman, L. and Winful, H. "Nonlinear dynamics of semiconductor laser arrays: a mean field model," *IEEE Journal of Quantum Electronics*, V30, pp. 1405-1416, 1994.

[22] Jones, C. R. and Kutz, J. N. "Stability of mode-locked pulse solutions subject to saturable gain: computing linear stability with the floquet–fourier–hill method," *J. Opt. Soc. Am. B*, V27, pp. 1184-1194, 2010.

[23] Doedel, E., Champneys, A., Dercole, F., Fairgrieve, T., Kuznetsov, Y., Oldeman, B., Paffenroth, R., Sandstede, B., Wang, X., and Zhang, C. "Auto: Software for continuation and bifurcation problems in ordinary differential equations," Technical report, Concordia University, Montreal, 2009.

[24] Trefethen, L. N. *Spectral methods in MATLAB*, SIAM, 2000.

[25] Williams, M. O. and Kutz, J. N. "Spatial mode-locking of light bullets in planar waveguide arrays," *Opt. Express*, V17, pp. 18320-18329, 2009.

[26] Wabnitz, S., Kodama, Y., and Aceves, A. B. "Control of optical soliton interactions," *Optical Fiber Technology*, V1, pp. 187 - 217, 1995.

[27] Sukhorukov, A. A. and Kivshar, Y. S. "Slow light bullets in arrays of nonlinear bragg-grating waveguides," In *Conference on Lasers and Electro-Optics/Quantum Electronics and Laser Science Conference and Photonic Applications Systems Technologies*, JWB82. Optical Society of America, 2006.

[28] Enns, R. H. and Rangnekar, S. S. "Bistable spheroidal optical solitons," *Phys. Rev. A*, V45, pp. 3354-3357, 1992.

[29] Blagoeva, A. B., Dinev, S. G., Dreischuh, A. A., and Naidenov, A. "Light bullets formation in a bulk media," *IEEE Journal of Quantum Electronics*, V 27, pp. 2060-2065, 1991.

[30] Kartashov, Y. V., Torner, L., and Christodoulides, D. N. "Soliton dragging by dynamic optical lattices," *Optics Letters*, V20, pp. 1378-1380, 2005.

[31] Królikowski, W., Trutschel, U., Cronin-Golomb, M., and Schmidt-Hattenberger, C. "Solitonlike optical switching in a circular fiber array," *Optics Letters*, V19, pp. 320-322, 1994.

[32] Meier, J., Stegeman, G. I., Christodoulides, D. N., Silberberg, Y., Morandotti, R., Yang, H., Salamo, G., Sorel, M., and Aitchison, J. S. "Beam interactions with a blocker soliton in one-dimensional arrays," *Optics Letters*, V30, pp. 1027-1029, 2005.

[33] Tanguy, Y., Ackemann, T., Firth, W. J., and Jäger, R. "Realization of a semiconductor-based cavity soliton laser," *Phys. Rev. Lett.*, V100, pp. 013907, 2008.

[34] Barland, S., Tredicce, J., Brambilla, M., Lugiato, L., Balle, S., Giudici, M., Maggipinto, T., Spinelli, L., Tissoni, G., Knödl, T., Miller, M., and Jäger, R. "Cavity solitons as pixels in semiconductor microcavities," *Nature*, V419, pp. 699-702, 2002.

[35] Taranenko, V. B. and Weiss, C. O. "Incoherent optical switching of semiconductor resonator solitons," *Applied Physics B*, V72, pp. 893-895, 2001.

[36] Barbay, S., Ménesguen, Y., Hachair, X., Lery, L., Sagnes, I., and Kuszelewics, R. "Incoherent and coherent writing and erasure of cavity solitons in an optically pumped semiconductor amplifier," *Optics Letters*, V31, pp. 1504-1506, 2006.

[37] Hachair, X., Furfaro, L., Javaloyes, J., Giudici, M., Balle, S., and Tredicce, J. "Cavity-solitons switching in semiconductor microcavities," *Phys. Rev. A*, V72, pp. 013815, 2005.